Seismic Performance of External Shear Keys in Box-Girder Railway Bridge Abutments

Mohamad Hasan Rajabpour [1], Ata Hojjat Kashani [1,*].

[1] Department of Civil Engineering, S.T.C, Islamic Azad University, Tehran (Iran),
mohamadhasan.rajabpour@iau.ir,
ata_hojat@aut.ac.ir

*Correspondence: ata_hojat@aut.ac.ir

Received: ; **Accepted:** ; **Published:**

Citation: RajabPour, M.H. Hojjat Kashani, A. (2025). Seismic Performance of External Shear Keys in Box-Girder Railway Bridge Abutments. INTERNATIONAL JOURNAL OF ADVANCED STRUCTURAL. https://doi.org/

Abstract:

Concrete box-girder railway bridges are among the most common bridge systems used to cross rivers and deep valleys where access beneath the deck is not possible. The typical span lengths in railway construction for this type of bridge system range from 55 to 110 meters. The lateral loads of the deck are transferred to the substructure through piers, elastomeric bearings, and lateral shear keys in the abutments.

The role of lateral shear keys in bridge piers and abutments of isolated bridge systems is to prevent deck collapse, reduce damage to substructure components, and act as structural fuses. Considering that the deck is often rigidly connected to the piers in most box-girder railway bridges, this study investigates the behavior of external shear keys in abutments of this bridge type under seismic forces.

Accordingly, one typical bridge with an integral concrete structure was selected, and Incremental Dynamic Analysis (IDA) was performed for two cases with and without lateral shear keys considering the transverse drift ratio failure criterion of up to 3% of pier height.

The results of analyses for 20 near-field and far-field ground motion records show that using external shear keys in abutments of box-girder concrete bridges improves the structural performance and reduces the probability of failure at the performance levels defined by the HAZUS guidelines, developed by FEMA.

Keywords: shear key, incremental nonlinear dynamic analysis, concrete box-girder bridge, railway

1. Introduction

Bridge structural systems generally have lower degrees of redundancy compared to buildings. In different bridge construction systems, these structures can be divided into main components and secondary components. The main components include the deck, abutments, piers, and foundations, while the secondary components consist of longitudinal shear keys, internal and external transverse shear keys, and railings. In bridge design, the main components are designed first, and then the secondary components are designed based on the geometry and the forces acting on the primary members. Among the secondary components, in bridges with isolated decks, longitudinal and transverse shear keys play a critical role in transferring lateral forces to the substructure and ensuring the deck's stability. These components are designed according to the seismic design approach adopted in bridge codes and seismic design guidelines.

Based on the damage observed in past earthquakes, Megally et al. [1] conducted large-scale experimental tests on several constructed models to investigate the seismic behavior of abutment shear keys with different reinforcement ratios under monotonic, cyclic quasi-static, and cyclic dynamic loads. The experimental results were then used to develop analytical behavioral models of shear keys for numerical studies. In their research, the performance of external shear keys as sacrificial fuses in abutments under earthquake-induced lateral loads was studied. Their results indicated that the truss mechanism design method (Strut and Tie) provides a more accurate estimation of the shear key's strength compared to the frictional shear design approach. Similary in other study, Bozorgzadeh et al. [2] examined previously built external shear key models and the provisions of the Caltrans Bridge Design Specifications, proposing an analytical model for calculating the capacity of external abutment shear keys. In their study, ten scaled models of shear keys (at a 1:2.5 scale ratio) were designed based on Caltrans requirements, constructed, and tested. Various failure modes including concrete cracking, steel yielding, bar buckling, and overall shear key failure were investigated. Their results emphasized the importance of considering a structural joint between the shear key and the abutment wall to allow sliding and shear-slip failure mechanisms. Accordingly, they developed a simple mechanical model for evaluating the shear capacity of keys with slip-type failures. This study employs this method (Strut and Tie) to establish the design parameters for the shear key.

In another study, Goel and Chopra [3] modeled bridges in three scenarios: (1) with linear shear key behavior, (2) with nonlinear shear key behavior, and (3) without shear keys, to assess the influence of shear keys on the seismic response of bridges crossing fault-rupture zones. Their findings revealed that the seismic responses of bridges with nonlinear shear keys could be approximated by those with linear shear keys or even without shear keys, although neglecting shear keys generally leads to overly conservative assessments of bridge responses under uniform ground motion. The concept of

incorporating transverse shear keys at abutments—or omitting them entirely in box girder railway bridges—was first introduced in this study.

Continuing prior research, Silva and colleagues [4] conducted tests on both internal and external shear keys, and based on their results, developed a two-spring hysteretic model to simulate the seismic behavior of shear keys. Similarly, Salveson and Fell [5] studied the effects of linear and nonlinear shear key behavior on bridge seismic response, finding that linear analysis results were surprisingly similar to those of nonlinear cases but more conservative.

In another investigation, Bi and Hao [6] modeled the seismic behavior of bridges with shear keys under earthquake loading. They found that shear keys significantly reduce torsional–transverse responses of bridges, leading to smaller impact forces and less structural damage. Moreover, they showed that neglecting shear keys in bridge analysis and design results in inaccurate seismic response predictions.

Numerous studies have also investigated bridge performance under various seismic conditions, including the soil–structure interaction effects. Meng et al. [7] examined the effects of shear keys and railway track systems on the behavior of simply supported bridges for high-speed trains subjected to transverse earthquake excitations. Their findings showed that the interaction between shear keys and elastomeric bearings significantly affects the bridge's seismic response by limiting the relative transverse displacements between the bridge girders and the piers after the initial impact gap closes, thereby reducing potential deck displacements.

To study the role and effects of external abutment shear keys in nonlinear incremental dynamic analysis (IDA), various failure criteria have been proposed in the literature. Mackie and Mackie and Stojadinović [8] defined displacement ductility and curvature ductility as damage criteria for two types of concrete bridge columns. Kwon and Elnashai [9] used top displacement and both displacement and curvature ductility as damage measures for post-1990 bridge designs. Banerjee and Shinozuka [10] defined a set of failure limits for single-column bridges considering rotational and curvature ductility. Likewise, Kim and Shinozuka [11] evaluated seismic performance using displacement ductility and identified four damage states for retrofitted bridges. The Caltrans [12] and AASHTO [13] codes also define steel and concrete yielding strains as bridge failure criteria. Shao and Xie [18] by investigating displacement ductility (μ_Δ), curvature ductility (μ_φ), and drift ratio(Δ/H) of columns and by unifying the limit states of engineering parameters based on the stresses developed in the longitudinal reinforcement, confined concrete of the column core, and unconfined cover concrete of circular reinforced concrete columns, proposed unified limit-state models for engineering parameters. The use of any of these limit states was shown to result in equivalent stress demands in the columns.

In this study, the limit states proposed by Shao and Xie [18] for displacement

ductility (μ_Δ), curvature ductility (μ_φ), and drift ratio (Δ/H) are adopted. By performing nonlinear pushover analyses in two loading directions, the elastic displacement points (Δ_y) of the columns is identified for 17 column specimens from railway box-girder bridges, covering a wide range of geometric dimensions and longitudinal reinforcement ratios. After determining the elastic displacement, nonlinear cyclic pushover analyses are conducted on the columns to derive unified limit states for the three engineering parameters. Based on the unified limits obtained for the engineering parameter of column drift ratio (Δ/H), incremental nonlinear dynamic analyses of the columns are subsequently performed.

2. Behavior and Design Methods of External Abutment Shear Keys

The external shear keys in abutments and pier caps of bridges are typically modeled and designed using two different approaches:

1. Sliding friction shear design, and
2. Truss mechanism (Strut-and-Tie) model.

Based on studies conducted by Megally et al. [1] the truss mechanism model provides a more accurate representation of the behavior of external shear keys. The concept is illustrated schematically in Figure 1.

In this method, the horizontal load is transferred through the shear key to the stem and then to the substructure. When the horizontal force is applied, a diagonal crack develops from the bottom edge of the shear key and propagates toward the upper toe of the foundation.

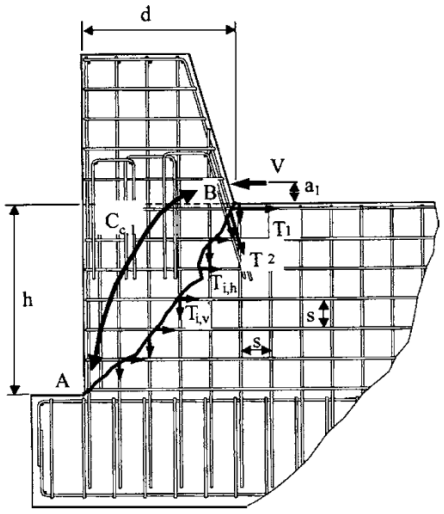

Fig. 1. Model schematic

Following the recommendations of Megally et al. [1] for using the truss mechanism model (strut and tie model), the shear resistance of external abutment shear keys can be formulated and calculated using the following relationships:

$$V_N = V_C + V_s$$

$$V_C = 0.2\sqrt{f_c'}.b.h$$

$$V_s = \left[A_{s,1}f_{y,1}h + A_{s,2}f_{y,2}d + n_h.A_{s,h}.f_{y,h}h\frac{h^2}{2S} + n_v.A_{s,y}.f_{y,y}h\frac{d^2}{2S}\right]\left(\frac{1}{h+a}\right)$$

(V_C) shear strength of concrete, (V_s) shear strength contributed by the reinforcing bars, (b) width of the abutment wall, (f_c'): compressive strength of concrete, (h): vertical distance of the diagonal crack formed in the abutment wall, (s): spacing

between horizontal and vertical reinforcing bars crossing the diagonal crack,

($A_{s,1}$): cross-sectional area of the first row of horizontal reinforcement in the abutment wall, ($A_{s,2}$): vertical reinforcement area of the first row in the shear key (inner side), ($A_{s,h}$): cross-sectional area of horizontal reinforcement crossing the diagonal crack, ($A_{s,y}$): cross-sectional area of vertical reinforcement crossing the diagonal crack, (n_h): number of horizontal reinforcing bars crossing the diagonal crack, (n_v): number of vertical reinforcing bars crossing the diagonal crack.

The reinforcement contribution V_s is related to the horizontal and vertical reinforcing bars that intersect the diagonal crack. The model effectively captures the nonlinear load–displacement behavior and energy dissipation capacity of the shear key during strong seismic events.

3. Geometric and Material Properties of the Sample Bridge

To evaluate the behavior of abutment shear keys, a sample concrete box-girder bridge with a constant-depth deck was selected. The geometric and material specifications of the bridge are presented in Table 1. This bridge is equipped with four external shear keys located on both sides of the abutments. The design of these shear keys follows the provisions of the AASHTO specifications and is based on a frictional design model. There is no clearance gap between the deck and the walls of the box-girder deck.

Table 1. Geometric and Material Properties of the Bridge

Parameter	Value
Total bridge length (m)	130
Span arrangement	35 + 60 + 35
Deck system	Constant-depth box girder
Box girder height	4 m
Deck top width	5.60 m
Box width	4.0 m
Maximum pier height (m)	25.50
Pier cross-section area dimensions	5.60 × 3.50 m
Pier thickness	40 cm
Shear key dimensions	70 × 70 × 180 cm
Concrete compressive strength (MPa)	30
Reinforcing steel yield strength (MPa)	420

The bridge is constructed using the balanced cantilever (progressive formwork) method, where the deck is cast segment by segment over the piers from both sides.

This bridge, which was selected for incremental nonlinear dynamic analysis (IDA), has a total length of 130 meters, consisting of three spans: a mid-span of 60 meters and two side spans of 35 meters each, as shown in Figure 2.

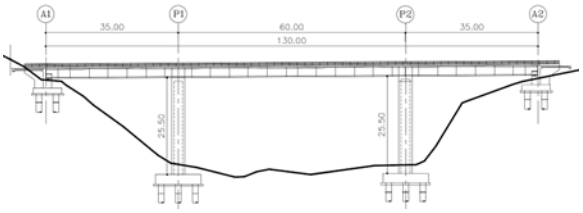

Fig. 2. Bridge longitudinal profile

The deck–pier connection is rigid (fixed), while the deck–abutment connection is made through elastomeric bearings.

At both ends of the bridge, the abutments act as simple supports. Each abutment is supported by six piles, each with a diameter of 1.20 meters. The hollow piers are also supported by twelve piles with the same diameter (1.20 m).

The external abutment shear keys have dimensions of 70 × 70 × 180 cm.

4. Finite Element Modeling of the Sample Bridge

The finite element (FE) model of the sample bridge was developed in Opensees (version 3.3.0) using the material models available in its internal library.

4.1 Material Modeling

For concrete elements, two material types were used: confined and unconfined concrete, both defined using the Concrete07 model in Opensees.

This model is based on the work of Chang and Mander [14], which defines the stress–strain relationships for confined and unconfined concrete derived from statistical analyses of cyclic compression test data.

For reinforcing steel, the Steel02 material model was adopted. This model, originally proposed by Filippou et al. [15], accurately simulates bilinear hysteretic behavior and isotropic strain hardening, capturing both yielding and post-yield stiffness in steel bars.

4.2 Deck Modeling

The bridge deck consists of a prestressed concrete box girder. According to bridge design philosophy in international standards (such as Caltrans and AASHTO), plastic hinges are expected to form at the bottom of piers, while the deck remains elastic during earthquakes.

Hence, the deck was modeled using ElasticBeamColumn elements to represent linear-elastic behavior.

Sensitivity, static, and nonlinear dynamic analyses were conducted to determine the optimal element discretization for the deck. Based on the height and width of the box girder and Caltrans code provisions, the effective deck width was taken equal to its actual structural width.

4.3 Pier Modeling

The piers are hollow box sections, rigidly connected at both ends (to the foundation and to the deck). To allow for the formation of distributed plasticity along the pier height, the DispBeamColumn element was used.

This element captures the nonlinear flexural behavior along the member length, enabling accurate simulation of plastic hinge development.

Since the foundations of the sample bridge are deep (pile-supported), the pile behavior was modeled using Hysteretic elements based on Choi's p–y curves [16], which represent nonlinear soil–pile interaction.

The behavior of piles in the active soil pressure zone is nonlinear and varies depending on depth and soil stiffness. The force–displacement relations from Choi's model were used to compute the active lateral stiffness of the piles, as summarized in Table3.

Table 2. stiffness of the piles

Effective Stiffness	$\mathbf{K_{eff}}$	7.0KN/mm/pile×number of piles
Initial Stiffness	$K_{1(a)}$	$2.333\times K_{eff}$
Displacement 1 at the top	$\Delta_{1(a)}$	7.62 mm
Second Stiffness	$K_{2(a)}$	$0.428\times K_{eff}$
Displacement 2 at the top	$\Delta_{2(a)}$	25.4 mm

4.4 Abutment and Backfill Modeling

The abutment model includes several components.
The backfill soil behind the abutment was modeled using HyperbolicGapMaterial, following the Shamsabadi et al [17] model. This material accounts for nonlinear passive and active soil resistance as a function of displacement.

The stiffness of the backfill, obtained from nonlinear dynamic analyses, is shown in Table 3.

Table 3. Backfill Stiffness Parameters

Parameter	Value
Abutment width (m)	5.60
Backfill height (m)	2.0
Effective backfill width (m)	5.60
Soil stiffness (kN/m)	313

4.5 Pile Modeling under Abutments

Similar to pier piles, the abutment piles were modeled using Hysteretic elements based on Choi's force–displacement relations, which account for nonlinear soil response under active pressure conditions.

4.6 Elastomeric Bearing Modeling

Elastomeric bearings (neoprene pads) are installed between the deck and abutments on both sides of the bridge.

These bearings resist lateral and vertical loads generated by seismic motions and deck gravity loads, transferring them to the abutment wall and then to the substructure.

Because elastomeric materials exhibit high resilience under seismic loads, their behavior was modeled using elasto-plastic elements with zero-length elements to represent the small deformation zone.

The stiffness of the elastomeric bearings was calculated using:

$$K = {}^{GA}/_{K}$$

Where:

(G) shear modulus of elastomer, (A) cross-sectional area of the elastomeric, (t) thickness of the elastomer layer.

The calculated stiffness for the neoprene bearings used in the bridge is presented in Table 4.

Table 4. Elastomeric Bearing Properties

Parameter	Value
Area (cm²)	50 × 60
Thickness (cm)	25
Shear modulus (MPa)	0.9
Stiffness (kN/m)	700

The frictional force between the deck and elastomeric bearings must be sufficient to prevent sliding.

According to bridge design codes, a minimum frictional force is required; if this is not met, the neoprene pads must be anchored with bolts and steel plates. The coefficient of friction (μ) between the deck and neoprene surface depends on the normal stress (σ) applied and is calculated as:

$$\mu = 0.05 + ({}^{0.4}/_{\sigma_m})$$

Where μ is the coefficient of friction and σ_m is the normal stress applied to the neoprene surface, with units of megapascals (MPa).

4.7 Shear Key Modeling

The external shear keys were modeled as zero-length elements, following the analytical relations developed by Megally et al. [1] The lateral stiffness of the external shear keys for the sample bridge is presented in Table 5.

Table 5. Shear Key Lateral Stiffness

Parameter	Stiffness (kN/m)
Initial stiffness	10,193
Secondary stiffness	322

5. Selection of Earthquake Records

To perform the required dynamic analyses on the bridge models, 20 pairs of near-field and far-field ground motion records were selected, as recommended by FEMA P695.

These records were downloaded from the PEER Ground Motion Database and cover a wide range of magnitudes, fault mechanisms, and site conditions to ensure reliable statistical representation of seismic effects.

The selected records and their specifications are presented in Table 6.

Table 6. Selected Earthquake Records

No.	Earthquake Name	Record No.	Year	Magnitude (Mw)
1	San Fernando	68	1971	6.6
2	Imperial Valley 6	174	1979	6.5
3	Loma Prieta	752	1989	6.9
4	Landers	900	1992	7.3
5	Northridge	960	1994	6.7
6	Kobe (Japan)	1116	1995	6.9
7	Hector Mine	1787	1999	7.1
8	Chi-Chi (Taiwan)	1485	1999	7.6
9	Düzce (Turkey)	1602	1999	7.4
10	Manjil (Iran)	1633	1990	7.4
11	Cape Mendocino	828	1992	7.0
12	Landers	879	1992	7.3
13	Northridge	1004	1994	6.7
14	Northridge	1048	1994	6.7
15	Northridge	1063	1994	6.7
16	Northridge	1086	1994	6.7
17	Kocaeli (Turkey)	1165	1999	7.5
18	Chi-Chi (Taiwan)	1503	1999	7.6
19	Düzce (Turkey)	1605	1999	7.4
20	Denali (Alaska)	2114	2002	7.9

These records were divided into two categories:

- Near-field records containing strong velocity pulses and directivity effects.
- Far-field records representing typical ground motions without near-fault effects.

Both record sets were used to assess the influence of ground motion type on the seismic performance and fragility behavior of the bridge models.

6. Developed Finite Element Models

To investigate the behavior of shear keys in box-girder railway bridges where the deck is rigidly connected to the piers and supported elastomerically on abutments two finite element models of the sample bridge were developed.

These two models were identical in every aspect except for the presence or absence of external shear keys on the abutments:

1. Model A: Bridge without external abutment shear keys,
2. Model B: Bridge with shear keys.

Since shear keys are considered secondary structural elements, it is expected that once they fail, the remaining primary components (piers, abutments, elastomeric bearings, and deck) will resist the lateral loads. Therefore, after the failure of the shear keys, both models should exhibit similar overall load-bearing mechanisms through their common components.

The results of the incremental nonlinear dynamic analysis (IDA) conducted on these two models were used to develop fragility curves and to assess the probability of failure under different seismic intensity levels.

7. Bridge Failure Criteria

Because modeling software cannot directly simulate all possible failure mechanisms in bridges, researchers often define limit states corresponding to the complete damage of key structural elements.

Failure modes in bridges can be described qualitatively, observationally, or quantitatively, depending on the study's objective. Each failure mode is characterized by specific damage criteria, which may apply to individual components (e.g., piers, bearings, abutments) or to the entire bridge system.

To generate fragility curves, it is essential to determine threshold values for each damage state ranging from no damage to total collapse. For reinforced concrete bridges, these thresholds are often associated with cracking, spalling, bar buckling, concrete crushing, or loss of load-carrying capacity.

According to the HAZUS 4.2 SP3 that is a geographic information system-based natural hazard analysis tool developed and freely distributed by the Federal Emergency Management Agency developed by FEMA, bridge damage is classified into four levels that are presented in Table 7.

Each damage state represents a higher degree of structural and functional degradation caused by seismic loading. Through incremental nonlinear dynamic analysis (IDA), the probability of reaching each of these performance levels can be estimated by generating response curves for the bridge.

Table 7 bridge damage is classified

Damage Level	Structural Behavior	Observable Damage
Slight	Elastic behavior with surface cracking	Fine flexural cracks; no permanent deformation
Moderate	Limited plastic deformation; onset of yielding	Concrete spalling; minor reinforcement yielding
Extensive	Plastic hinge formation; partial bar buckling	Deep cracking, permanent deformation, stiffness loss
Complete	Structural instability; shear or flexural failure	Deck collapse, pier failure, component separation

Common engineering parameters indicators used for assessing damage in integral bridges include:

- displacement ductility (μ_Δ)
- curvature ductility (μ_φ),
- drift ratio (Δ/H)

After identifying the unified seismic performance levels using different engineering parameters, the lateral Drift ratio ductility (Δ/H) of the bridge pier was selected as controlling parameter for performing Incremental Dynamic Analysis (IDA), using the values presented in Table 8. These drift ratio thresholds were adopted in this study to define the four seismic performance levels of the bridge models, serving as the basis for fragility curve development.

Table 8. Performance Levels Based on Transverse Pier Drift Ratio

Performance Level	Slight	Moderate	Extensive	Complete
Transverse displacement ratio (% of pier height)	0.75	1.5	2.0	3.0

8. Conducted Analyses

One of the most precise and advanced methods for performance-based seismic assessment and for determining limit states of structural components is the Incremental Dynamic Analysis (IDA) method.

The results obtained from IDA provide valuable insight into the fragility behavior of both primary and secondary structural elements, offering comprehensive information about the bridge response under varying earthquake intensities.

8.1 Methodology

In this method, a series of real ground motion records are applied to the nonlinear structural model of the bridge. The intensity of each record is gradually scaled up until the structure reaches its limit state or experiences collapse.

The structural responses such as lateral displacement, stiffness degradation, and energy dissipation are recorded for each intensity level. These data are then used to generate IDA curves, which describe how the bridge performance evolves as seismic intensity increases.

The probability of exceeding each damage state is determined by comparing the response quantities with the damage thresholds defined previously (Table 8).

8.2 Analysis Procedure

In this study, the Hunt–Fill method, proposed by Vamvatsikos [19], was adopted for the IDA procedure.
This method provides a balance between accuracy and computational efficiency, as it minimizes the number of required iterations by adaptively scaling the ground motion records based on the previous response level.

For each of the 20 selected ground motion records, the scaling factors were progressively increased until one of the failure criteria was reached:

1. Transverse pier displacement ratio exceeding 3%, or
2. Reduction in structural stiffness exceeding 20% of the initial value.

When either of these criteria was satisfied, the analysis for that record was terminated, and the ultimate failure point was recorded.

8.3 IDA Results

The IDA curves for the 20 selected near-field and far-field ground motions were generated for both bridge configurations.

Figures 3 and 4 present the resulting IDA response envelopes.

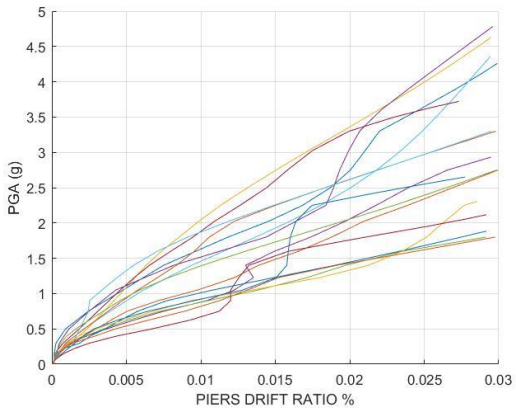

Fig. 3. Bridge without external shear keys

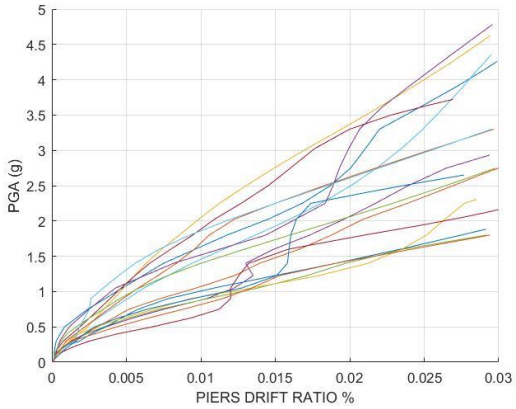

Fig. 4. Bridge with external shear keys

From the analysis results, it was observed that the stiffness degradation parameter is a reliable indicator of structural performance during the analysis.
In addition, the transverse displacement ratio at the pier tops was found to be an effective measure for defining damage levels and failure states in the developed finite element models.

9. Fragility Curves and Comparative Results

Developing fragility curves is one of the most effective methods for quantitatively comparing the seismic behavior of structures and evaluating the vulnerability of structural components under earthquake excitation.

A fragility curve represents the probability that the seismic demand on a structure (e.g., displacement, acceleration) will exceed its capacity for a given level of ground motion intensity.

These curves are typically expressed in terms of Peak Ground Acceleration (PGA) or Spectral Acceleration (Sa), and are characterized by a lognormal cumulative distribution function defined by two parameters:

$$P[\,\text{Damage} \geq \text{LS} \mid \text{PGA}\,] = \Phi\left(\frac{\ln(\text{PGA}) - \ln(\mu)}{\beta}\right)$$

Where:

- P: probability that seismic demand exceeds capacity;
- Φ: standard normal cumulative distribution function;
- μ: median value of PGA corresponding to the onset of a given damage state;
- β: logarithmic standard deviation representing the variability in that damage state.

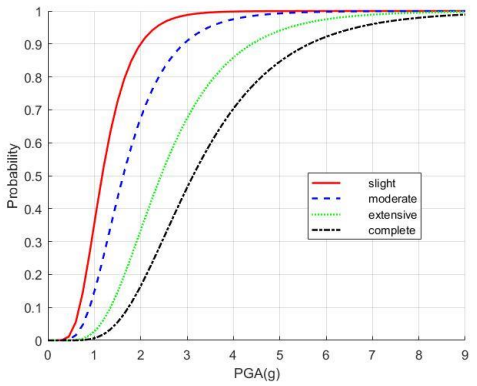

Fig. 5. Fragility curves for Bridge without external shear keys

Each curve represents the cumulative probability of damage exceeding a specific level (Slight, Moderate, Extensive, Complete) as a function of PGA.

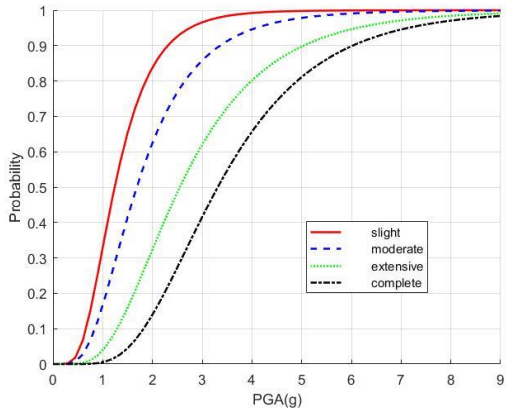

Fig. 6. Fragility curves for Bridge with shear keys

9.4 Comparative Analysis

For both bridge configurations, fragility curves were compared across the four damage states that are shown in figure 6.

The results demonstrated that the bridge with external shear keys exhibited a lower probability of exceeding all four damage states compared to the bridge without shear keys.

This indicates that the presence of external abutment shear keys significantly enhances the overall seismic performance and

9.1 Damage Measure and Limit States

In this study, transverse pier displacement was selected as the damage index, in accordance with the previously defined damage thresholds (Table 8).

Using the IDA results, the median PGA values (μ) and the corresponding logarithmic standard deviations (β) were determined for each of the four damage states (Slight, Moderate, Extensive, Complete).
These parameters were then used to generate the fragility curves for the two bridge models:

9.2 Statistical Parameters

The computed statistical parameters for each damage level are summarized in Table 9.

Table 9. Median and Logarithmic Standard Deviation Values

Damage Level	Slight	Moderate	Extensive	Complete
Median (μ)	0.1559	0.4842	1.0153	1.1407
Log Std. Dev. (β)	0.4178	0.4600	0.4550	0.4591

9.3 Fragility Curves

Using these statistical parameters, the fragility curves were derived for both bridge configurations, which are shown in figure 5 and 6:

the seismic performance of concrete box-girder railway bridges.

2. The probability of failure across all four performance levels was noticeably lower for the model with shear keys compared to the model without them.

3. External shear keys act as energy-dissipating fuse elements, helping to transfer lateral forces from the deck to the substructure while limiting deck displacement and reducing damage to other structural components.

4. The use of external shear keys also reduces the likelihood of unseating or collapse of the deck during severe earthquakes.

5. The findings confirm that proper design and detailing of external abutment shear keys—as recommended in Caltrans can play a crucial role in enhancing the seismic resilience of railway bridges with integral box-girder systems.

Overall, the results show that incorporating external shear keys in the abutment design leads to improved structural behavior, lower damage probabilities, and greater safety margins under seismic loading.

References:

[1]. Megally, S. H., Silva, P. F., & Seible, F. (2002). Seismic response of external sacrificial shear keys. Report No. SSRP-2001/23, Department of Structural Engineering, University of California, San Diego, 198 pp.

[2]. Bozorgzadeh, A., Megally, S., Restrepo, J. I., & Ashford, S. A. (2006). Capacity

reduces the vulnerability of the bridge system.

10. Conclusions

In this study, two finite element models of a concrete box-girder railway bridge were developed to investigate the influence of external abutment shear keys on seismic performance.
The two models were identical in all aspects except for the presence or absence of external shear keys at the abutments.

A series of Incremental Dynamic Analyses (IDA) were conducted using 20 near-field and far-field ground motion records recommended by FEMA P695.

For each model, fragility curves corresponding to the four performance levels (Slight, Moderate, Extensive, and Complete) were derived based on the IDA results.

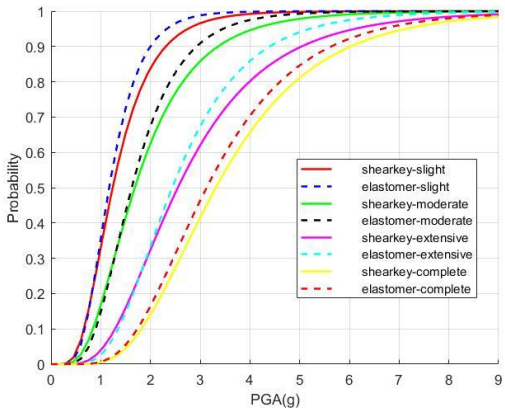

Fig. 7. fragility curves for both models

A comparative evaluation of the two bridge configurations led to the following conclusions:

1. The inclusion of external shear keys in abutments significantly improves

Infrastructure Engineering, 6(1–2), 159–178. https://doi.org/10.1080/15732470802663870

[10]. Banerjee, S., & Shinozuka, M. (2007). Nonlinear static procedure for seismic vulnerability assessment of bridges. Computer-Aided Civil and Infrastructure Engineering, 22(4), 293–305. https://doi.org/10.1111/j.1467-8667.2007.00486.x

[11]. Kim, S. H., & Shinozuka, M. (2004). Development of fragility curves of bridges retrofitted by column jacketing. Probabilistic Engineering Mechanics, 19(1–2), 105–112. https://doi.org/10.1016/j.probengmech.2003.11.009

[12]. Caltrans. (2014). LRFD Bridge Design Specifications. California Department of Transportation.

[13]. FEMA. (2019). Hazus Earthquake Model Technical Manual (Version 4.2 SP3). Federal Emergency Management Agency.

[14]. Chang, G. A., & Mander, J. B. (1994). Seismic energy-based fatigue damage analysis of bridge columns: Part 1 – Evaluation of seismic capacity. State University of New York at Buffalo.

[15]. Filippou, F. C., Popov, E. P., & Bertero, V. V. (1983). Effects of bond deterioration on hysteretic behavior of reinforced concrete joints. University of California, Berkeley.

[16]. Choi, E. (2002). Seismic analysis and retrofit of mid-America bridges. Georgia Institute of Technology.

[17]. Shamsabadi, A., Rollins, K. M., & Kapuskar, M. (2007). Nonlinear soil–abutment–bridge structure interaction for seismic performance-based design. Journal of geotechnical and geoenvironmental engineering, 133(6), 707-720. https://doi.org/10.1061/(ASCE)1090-0241(2007)133:6(707)

[18]. Shao, Y., & Xie, Y. (2024). Unified seismic capacity limit state models of reinforced evaluation of exterior sacrificial shear keys of bridge abutments. Journal of Bridge Engineering, 11(5), 555–565. https://doi.org/10.1061/(ASCE)1084-0702(2006)11:5(555)

[3]. Goel, R. K., & Chopra, A. K. (2008). Role of shear keys in seismic behavior of bridges crossing fault-rupture zones. Journal of Bridge Engineering, 13(4), 398–408.https://doi.org/10.1061/(ASCE)1084-0702(2008)13:4(398)

[4]. Silva, P. F., Megally, S., & Seible, F. (2009). Seismic performance of sacrificial exterior shear keys in bridge abutments. Earthquake Spectra, 25(3), 643–664. https://doi.org/10.1193/1.3155405

[5]. Salveson, M. W., & Fell, B. V. (2011, April). Effect of abutment shear keys on the seismic response of bridges. In Structures Congress 2011 (pp. 265–275). American Society of Civil Engineers. https://doi.org/10.1061/41171(401)24

[6]. Bi, K., & Hao, H. (2015). Modelling of shear keys in bridge structures under seismic loads. Soil Dynamics and Earthquake Engineering, 74, 56–68.https://doi.org/10.1016/j.soildyn.2015.03.013

[7]. Meng, D., Chen, S., Yang, M., & Hu, S. (2021). Effects of shear keys and track systems on the behavior of simply-supported bridges for high-speed trains subjected to transverse earthquake excitations. Advances in Structural Engineering, 24(12), 2607–2621. https://doi.org/10.1177/13694332211007398

[8]. Mackie, K., & Stojadinović, B. (2001). Probabilistic seismic demand model for California highway bridges. Journal of Bridge Engineering, 6(6), 468–481. https://doi.org/10.1061/(ASCE)1084-0702(2001)6:6(468)

[9]. Kwon, O. S., & Elnashai, A. S. (2010). Fragility analysis of a highway over-crossing bridge with consideration of soil–structure interaction. Structure and

concrete bridge columns. In Canadian Society of Civil Engineering Annual Conference (pp. 435–452). Springer, Cham. https://doi.org/10.1007/978-3-031-34027-7_29

[19]. Vamvatsikos, D., & Cornell, C. A. (2004). Applied incremental dynamic analysis. Earthquake Spectra, 20(2), 523–553. https://doi.org/10.1193/1.1737737